rate constants are reduced by 20-30% when the reactants are deuterated (see Table I). This indicates that the proton on the oxygen donor atom plays an important role in the reaction. At least one proton is absolutely necessary for the hydroxyl group in boric acid to be released as a water molecule and the more protonated ligands react more rapidly. In fact, the difference in reactivity between Hipt and H_2cht^{2-} is significant.

Concerning a number of reaction systems, it has been demonstrated that activation volumes are very useful for diagnosing the reaction mechanism.[32] We shall discuss the pressure effect of the present reactions. The experimentally obtained activation volume, ΔV_f^*, for the forward reaction is given as follows for each respective step: for the Hipt and H_2cht^{2-} systems $\Delta V_f^* = \Delta V^{**}$ and for the H_2res^{2-} system $\Delta V_f^* = \Delta V_1^\circ + \Delta V_2^\circ + \Delta V^{**}$, where ΔV_1° and ΔV_2° are the reaction volumes for step I and step II, respectively, and ΔV^{**} is the activation volume for the rate-determining step.

The fact that the boron-oxygen bond lengths are 137 pm in $B(OH)_3$ and 148 pm in $B(OH)_4^-$, respectively,[33] implies that the structural change from the trigonal boric acid to the tetrahedral unchelated complex causes an increase in the boron-oxygen bond length. On the other hand, the entrance of a hydroxyl group into the inner sphere of boric acid invokes a volume decrease. The latter volume-decreasing effect would prevail, and consequently the volume of activation is negative for the forward reactions of eqs 1 and 2 (see Table I). Furthermore, large negative values of entropy of activation are in accordance with considerably large negative volumes. Thus, the forward reactions of eqs 1 and 2 should proceed by the mechanism with an associative mode.

We can postulate that the sum of volume changes ($\Delta V_1^\circ + \Delta V_2^\circ$) for steps I and II in the H_2res^{2-} reaction is almost equal to the overall reaction volume ($\Delta V^\circ = \Delta V_f^* - \Delta V_d^* = -2.8 \pm 0.7$ cm^3 mol^{-1}) for the Hipt reaction because of their similarity (see Scheme I). ΔV^{**} for step III in the H_2res^{2-} reaction should then be equal to $\Delta V_f^* - (\Delta V_1^\circ + \Delta V_2^\circ) = 3.9 - (-2.8) = +6.7$ cm^3 mol^{-1}. This second chelate-forming step (III) corresponds to the ring closure of the tetrahedral complex. Therefore, at this stage it is worthwhile to compare step III in Scheme I to the complexation of a tetrahedral metal ion such as the beryllium(II) ion. The activation volume for the reaction between the tetrahedral beryllium(II) ion and Hipt in aqueous solution is negative (-7.1 cm^3 mol^{-1}),[18] while that of the second chelate-ring closure in the H_2res^{2-} reaction is positive (+6.7 cm^3 mol^{-1}) as previously estimated. The chelate-forming six-membered-ring closure of the small central atom such as boron is sterically difficult due to strain. This may result in a volume increase of the transition state and is the reason that reaction 3 is much slower compared with reactions 1 and 2.

The volume of activation for the reverse reaction, i.e. the complex dissociation reaction, corresponds to the difference in partial molar volume between a transition state and a final state. The dissociation reaction involves a ring-opening step as a preequilibrium, as shown in Scheme I. In step II for the H_2cht^{2-} system an oxonium ion (H_3O^+) is the entering ligand and the leaving group is the hydroxyl group in H_2cht^{2-}. ΔV_2° for step II of this reaction should then be positive because of charge neutralization during the reaction. Therefore, the activation volume for the activation process should be more negative than the overall activation volume (-6.3 cm^3 mol^{-1}) for the dissociation reaction. The difference between the overall reaction volumes for reactions 1 and 2 is -6.2 cm^3 mol^{-1}, which may correspond to the electrostriction due to the released proton.[34] Thus, the mechanisms may be substantially the same for both reactions 1 and 2. In conclusion, both the forward and reverse processes for reactions 1 and 2 should be activated via the associative mode.

Acknowledgment. We thank Dr. Shoji Motomizu and Dr. Mitsuko Oshima (Okayama University) for donating the H-resorcinol reagent. K.I. gratefully acknowledges financial support by a grant from the Kurata Foundation. This work was supported by the Grants-in-Aid for Scientific Research (No. 62470041 and No. 63740335) and for Scientific Research on Priority Areas (No. 02245106) from the Ministry of Education, Science, and Culture of Japan.

Registry No. Hipt, 499-44-5; $B(OH)_3$, 10043-35-3; chromotropic acid, 148-25-4; H-resorcinol, 3627-01-8.

Supplementary Material Available: Observed rate constants at various temperatures and pressures (Tables SI-SX) (10 pages). Ordering information is given on any current masthead page.

(32) (a) van Eldik, R., Ed. *Inorganic High Pressure Chemistry: Kinetics and Mechanisms*; Elsevier: Amsterdam, 1986. (b) van Eldik, R.; Asano, T.; le Noble, W. J. *Chem. Rev.* **1989**, *89*, 549.
(33) Christ, C. L.; Clark, J. R.; Evans, H. T. *Acta Crystallogr.* **1958**, *11*, 761.
(34) Millero, F. J. *Chem. Rev.* **1971**, *71*, 147. The partial molar volume of H^+ is ca. -4.5 cm^3 mol^{-1}.

Contribution from the Department of Chemistry, University of Rhode Island, Kingston, Rhode Island 02881

Reduction of the Tetrahydroxoargentate(III) Ion by Thiocyanate in Aqueous Alkaline Media

Louis J. Kirschenbaum* and Yunfu Sun

Received August 14, 1990

The reduction of $Ag(OH)_4^-$ by thiocyanate ion in the range $5 \times 10^{-4} \le [SCN^-] \le 0.25$ M was studied in aqueous alkaline media at 25 °C and $\mu = 1.2$ M by stopped-flow spectrophotometry. At $[SCN^-] \le 0.01$ M, the reaction was found to be first-order in each reactant, with an apparent second-order rate constant of 21.7 ± 0.3 M^{-1} s^{-1}. At higher thiocyanate concentrations, silver(III) disappearance continues to appear pseudo first order, but the thiocyanate dependence becomes complex. Oxidation products are SO_4^{2-}, OCN^-, and (at high SCN^- only) cyanide ion. A mechanism is proposed consisting of a series of two-electron redox steps. Competition between SCN^- and reaction intermediates for remaining silver(III) accounts for changes in both rate and product distribution. The activation enthalpy and entropy for the initial step are 28.3 ± 1.2 kJ mol^{-1} and -129 ± 7 J mol^{-1} K^{-1} respectively. Numerical simulation and reaction with potential intermediates have been used to support the conclusions.

Introduction

The oxidation of thiocyanate is often complicated by the varied oxidation states of sulfur and the relative redox instability of cyanide, which is a potential product. Sulfate and cyanide are often the major products,[1-4] but additional species can be found, including $(SCN)_2$,[5] $S(CN)_2$,[6] and $OSCN^-$,[7] which hydrolyze under relevant conditions to sulfate and cyanide or cyanate. Under

(1) Stanbury, D. M.; Wilmarth, W. K.; Khalaf, S.; Po, H. N.; Byrd, J. E. *Inorg. Chem.* **1980**, *19*, 2715.

0020-1669/91/1330-2360$02.50/0

appropriate conditions, cyanide can be oxidized to cyanate[8] or to carbonate and ammonia.[9]

One-electron-transfer processes involve $SCN^\bullet$ and $(SCN)_2^{\bullet-}$ radicals,[1,2] but the large $SCN^\bullet/SCN^-$ potential[2] makes this path vulnerable. A two-electron-transfer mechanism with XSCN (X = Cl, Br)[4] or SCN^+[10] as intermediates have also been proposed. Transfer of two electrons may involve intermediates such as $OSCN^-$, $OOSCN^-$, $OOS(O)CN^-$, $OS(O)CN^-$, $OS(O)_2CN^-$ and their acids.[11-13] All of these intermediates hydrolyze or react with each other, giving sulfate and cyanate or cyanide as final products.

SCN^- is also a good complexing agent, binding preferably at the sulfur end to square-planar 4d and 5d metals. One of the few cases where a five-coordinate intermediate has been directly observed in an associative ligand replacement reaction involves the axial attack of SCN^- on $AuCl_4^-$.[14]

The hypervalent tetrahydroxoargentate(III) ion is a strong oxidizing agent. It is most often reduced to silver(I),[15,16] but sometimes to AgO[17] and even to metallic silver.[18] Silver(III) redox reactions can involve either one- or two-electron-transfer processes, depending on the reductant. Oxidation of $Mn(CN)_6^{4-}$ and $W(CN)_8^{4-}$,[19] HO_2^-,[20] $Fe(CN)_6^{3-}$ and MnO_4^{2-},[21] and 4-*tert*-butylphenolate anion[22] proceed via one-electron mechanisms, with Ag(II) intermediates. The reduction of arsenite,[14] sulfite,[16] and hypophosphite[23] oxoanions involve a one-step oxygen atom transfer, while the reduction of other species (including azide,[24] thiourea,[25] thiosulfate,[26] and mandelate ion[27]) occur as simultaneous two-electron transfers.

Silver(III) is a low spin d^8 system and its square-planar geometry provides $Ag(OH)_4^-$ with the opportunity to undergo inner-sphere redox either within a five-coordinate intermediate or after replacement of bound hydroxide ligands. In this paper, we present the results of the study of the reaction of $Ag(OH)_4^-$ with thiocyanate ion. Although no direct evidence for silver(III)–SCN^- association is obtained, we find that oxidized sulfur species are sufficiently reactive that multistep redox (toward SO_4^{2-}) occurs even at excess $[SCN^-]$.

Table I. Reaction Stoichiometry at Excess SCN^-[a]

$10^3[Ag(III)]_0$, M	$10^3[SCN^-]_0$, M	$[SCN^-]_0/[Ag(III)]_0$	$\Delta[SCN^-]/\Delta[Ag(III)]$
1.61	4.8	3.0	1.1
1.61	4.0	2.5	1.1
1.61	3.2	2.0	1.0
1.61	2.4	1.5	1.1
1.61	1.6	1.0	*b*

[a] μ = 1.2 M; $[OH^-]$ = 1.2 M. [b] No thiocyanate remains.

Experimental Section

Reaction Solutions. All stock solutions were made from doubly distilled water. Thiocyanate solutions were freshly made by dissolving accurately weighed reagent grade NaSCN (Baker & Adamson) in 1.2 M NaOH and/or 1.2 M $NaClO_4$. Stock NaOH solutions were prepared from 50% low carbonate NaOH (Fisher). $NaClO_4$ was prepared from NaOH and $HClO_4$ (Fisher).[28]

$Ag(OH)_4^-$ solutions were prepared by electrolysis of silver foil (Handy and Harman) in 1.2 M NaOH solution as described previously.[16,29]

Kinetics. Kinetic measurements were carried out with an Aminco-Morrow stopped-flow apparatus coupled to a Tandy TRS-80 microcomputer[15] at 25 °C and μ = 1.2 M unless noted otherwise. A large excess of reductant was used throughout the experiments. The reduction of $Ag(OH)_4^-$ was followed as decrease in absorbance at 267 nm where $Ag(OH)_4^-$ has a molar extinction coefficient of 1.17×10^4 M^{-1} cm^{-1}. The kinetic data were processed with the program Kinfit (On-Line Instrument Systems Inc, Jefferson, GA) after transfer to PC media.

Product Analysis. The qualitative analysis of sulfate was carried out by precipitation with $Ba(NO_3)_2$ (Mallinckrodt); the precipitate was identified by its IR spectrum. UV spectroscopy was used to investigate the possible production of $(SCN)_2$ (λ_{max} = 295 nm) after extraction into organic phase. The Jackson modification of Nessler's reagent was used to test for ammonia.[30a] Cyanide analysis was by the picric acid method.[30b]

Stoichiometry. When excess thiocyanate is used, the SCN^- remaining after reaction was analyzed spectrophotometrically by forming a complex with excess ferric ion and measuring the absorbance of the complex at 458 nm.[31] The reaction mixtures were first filtered to remove AgSCN precipitate and acidified to pH 3–5.

Results

Identification of Products. For $[SCN^-] \leq 0.01$ M, the reduction of $Ag(OH)_4^-$ by thiocyanate gives a white precipitate as the final silver-containing product. The precipitate dissolves in excess NaSCN, suggesting that it is AgSCN. The IR spectrum of the precipitate confirmed this identification.

Addition of $Ba(NO_3)_2$ indicated that sulfate was the only detectable sulfur-containing oxidation product at lower thiocyanate concentration. $BaSO_4$ was confirmed from IR spectra,[16] which were devoid of $BaSO_3$ peaks. The presence of significant amounts of $(SCN)_2$ and $S(CN)_2$ can be ruled out since the carbon tetrachloride extraction did not yield either of these two species in the organic phase. The absence of a peak at 235 nm and the inactivity of product solutions toward iodide rule out the presence of hypothiocyanite, $OSCN^-$.[7] At this SCN^- concentration range, no cyanide was detected by the picric acid test. Nessler's reagent gave no indication of NH_3 when added directly to the (alkaline) reaction mixture. However, after the solution was acidified and brought back to basic, Nessler's test gave a cloudy reddish brown solution, confirming the presence of ammonia. This indicates that cyanate (which hydrolyzes in acid) is an oxidation product.

At higher thiocyanate concentrations, both cyanide and cyanate were detected, and the mixture was clear, probably because of the formation of anionic Ag(I) complexes with excess SCN^- and

(2) Nord, G.; Pedersen, B.; Farver, O. *Inorg. Chem.* **1978**, *17*, 2233.
(3) Briot, G. T.; Smith, R. H. *Aust. J. Chem.* **1973**, *26*, 1863.
(4) Elding, L.; Grōning, A.-B.; Grōning, V. *J. Chem. Soc., Dalton Trans.* **1981**, 1093.
(5) Davies, G.; Watkins, K. O. *J. Phys. Chem.* **1970**, *74*, 3308.
(6) Stedman, G.; Whimcup, P. A. E. *J. Chem. Soc. A* **1969**, 1145.
(7) Thomas, E. L. *Immunol. Ser.* **1985**, *27*, 31.
(8) Masson, O. *J. Chem. Soc.* **1907**, *91*, 1449.
(9) Kolthoff, I. M.; Stenger, V. A. *Volumetric Analysis*; Interscience Publishing, Inc.: New York, 1967; Vol. 2, p 267.
(10) Treindl, L.; Fico, M. *Collect. Czech. Chem. Commun.* **1969**, *34*, 2873.
(11) Luo, Y.; Orbán, M.; Kustin, K.; Epstein, I. R. *J. Am. Chem. Soc.* **1989**, *111*, 4541.
(12) Wilson, I. R.; Harris, G. M. *J. Am. Chem. Soc.* (a) **1960**, *82*, 4515; (b) **1961**, *83*, 286.
(13) Simoyi, R. H.; Epstein, I. R.; Kustin, K. *J. Phys. Chem.* **1989**, *93*, 2792.
(14) Hall, A. J.; Satchell, D. P. N. *J. Chem. Soc., Dalton Trans.* **1977**, 1403.
(15) (a) Kirschenbaum, L. J.; Rush, J. D. *Inorg. Chem.* **1983**, *22*, 3304. (b) Kirschenbaum, L. J.; Rush, J. D. *J. Am. Chem. Soc.* **1984**, *106*, 1003.
(16) Kirschenbaum, L. J.; Kouadio, I.; Mentasti, E. *Polyhedron* **1989**, *8*, 1299.
(17) Rush, J. D.; Kirschenbaum, L. J. *Polyhedron* **1985**, *4*, 1573.
(18) Kirschenbaum, L. J. *J. Inorg. Nucl. Chem.* **1976**, *38*, 881.
(19) Borish, E. T.; Kirschenbaum, L. J.; Mentasti, E. *J. Chem. Soc., Dalton Trans.* **1985**, 1789.
(20) Borish, E. T.; Kirschenbaum, L. J. *J. Chem. Soc., Dalton Trans.* **1983**, 749.
(21) Kirschenbaum, L. J.; Borish, E. T.; Rush, J. D. *Isr. J. Chem.* **1985**, *25*, 159.
(22) Kirschenbaum, L. J.; Panda, R. K. *J. Chem. Soc., Dalton Trans.* **1989**, 217.
(23) Mehrotra, R. N.; Kirschenbaum, L. J. *Inorg. Chem.* **1989**, *28*, 4327.
(24) Borish, E. T.; Kirschenbaum, L. J. *Inorg. Chem.* **1984**, *23*, 2355.
(25) Kirschenbaum, L. J.; Panda, R. K. *Polyhedron* **1988**, *7*, 2753.
(26) Rush, J. D.; Kirschenbaum, L. J. *Inorg. Chem.* **1985**, *24*, 744.
(27) Kouadio, I.; Kirschenbaum, L. J.; Mehrotra, R. N.; Sun, Y. *J. Chem. Soc., Perkin Trans. 2* **1990**, 2123.
(28) Kouadio, I.; Kirschenbaum, L. J.; Mehrotra, R. J. *J. Chem. Soc., Dalton Trans.* **1990**, 1929.
(29) Kirschenbaum, L. J.; Ambrus, J. H.; Atkinson, G. *Inorg. Chem.* **1973**, *12*, 2832.
(30) Snell, P.; Snell, C. T. *Colorimetric Methods of Analysis*; 3rd ed.; D. Van Nostrand Company, Inc.: Toronto, 1949; Vol. 2: (a) p 814; (b) p 864.
(31) Kolthoff, I. M.; Sandell, E. B.; Meehan, E. J.; Bruckenstein, S. *Quantitative Chemical Analysis*, 4th ed.; The Macmillan Company Collier-Macmillan Limited: London, 1969; p 1049.

Table II. Pseudo-First-Order Rate Constants for Thiocyanate Oxidation

	OH^- concn, M							
$[SCN^-]$, M	0.12	0.3	0.6	0.9	1.2	k_{obsd}	k_{calc}[a]	k_{simul}[b]
0.0005	0.021	0.0242	0.0266	0.0204	0.0294	0.0243	0.0248	0.0246
0.001	0.034	0.0330	0.0337	0.0309	0.0404	0.0344	0.0357	0.0365
0.0025	0.074	0.0724	0.0705	0.0681	0.0688	0.0709	0.0682	0.0705
0.005	0.133	0.128	0.122	0.125	0.126	0.127	0.122	0.125
0.0075	0.174	0.176	0.187	0.168	0.174	0.176	0.177	0.173
0.01	0.215	0.234	0.228	0.234	0.228	0.228	0.231	0.223
0.025	0.516	0.526	0.523	0.491	0.487	0.509	(0.556)	0.472
0.05	0.818	0.84	0.879	0.834	0.894	0.853	(1.10)	0.815
0.075	1.02	1.05	1.17	1.16		1.10	(1.64)	1.11
0.1	1.29	1.33	1.44	1.50		1.39	(2.18)	1.42
0.15			1.98			1.98	(3.26)	1.97
0.2			2.48			2.48	(4.35)	2.49
0.25	2.74	2.88	2.87	3.00		2.87	(5.43)	2.90

[a] From linear fit of data at $[SCN^-] \leq 0.01$ M, $k_{calc} = 0.014 + 21.7 \times [SCN^-]$. Values in parentheses are for $[SCN^-]$ beyond the linear range. [b] First-order fit of disappearance of 5×10^{-5} M $Ag(OH)_4^-$ via reactions 2–7 after simulation with $k_1 = 6.0$, $k_2 = 4 \times 10^5$, $k_3 = 1 \times 10^4$, and $k_4 = 1 \times 10^5$.

CN^-. Neither solid silver oxide nor metallic silver was detected under any conditions.

It should be noted that, in order to produce detectable quantities of products, the concentration of silver(III) used for these product analyses and the stoichiometry experiments was about an order of magnitude greater than in the kinetic runs and $[OH^-]$ was maintained at 1.2 M.

Stoichiometry. For the thiocyanate oxidation reaction, stoichiometry measurements at excess Ag(III) were not possible. Even under the most favorable conditions, the maximum concentration of $Ag(OH)_4^-$ attainable is about 3×10^{-3} M in 1.2 M NaOH. Thus in order to maintain excess Ag(III), the concentration of thiocyanate must be so low that the redox reaction is too slow to be distinguishable from the spontaneous decomposition of Ag(III). At small excess of thiocyanate, unreacted SCN^- was measured spectrophotometrically as the $FeSCN^{2+}$ complex. The results are listed in Table I. The $\Delta[SCN^-]:\Delta[Ag(III)]$ ratio close to 1.1:1 is consistent with reaction 1, which predicts a ratio of 1.25:1.

$$4Ag(OH)_4^- + 5SCN^- \rightarrow 4AgSCN + SO_4^{2-} + OCN^- + 5H_2O + 6OH^- \quad (1)$$

The low experimental value is consistent with some spontaneous Ag(III) decomposition.

While stoichiometry measurements are impractical at high excess of thiocyanate the detection of cyanide points to a decrease in the extent of oxidation with increasing $[SCN^-]$. This is as would be expected for a multistep reaction as the initial step(s) deplete the limiting reagent.

Kinetics. The kinetic runs were carried out at 25 °C and 1.2 M ionic strength with the initial Ag(III) concentration typically around 5×10^{-5} M and SCN^- in large excess. Most reactions were followed as the decrease of Ag(III) absorbance at 267 nm. The data gave a satisfactory fit to a first-order rate law for all concentrations. The pseudo-first-order rate constant, k_{obsd}, was not affected by variation of the monitoring wavelength in the region (267 nm $< \lambda <$ 320 nm) where silver(III) can be measured. Extending the range of higher λ gave no indication of formation of reaction intermediates.

Values of k_{obsd} are listed in Table II. At low SCN^- concentration ($[SCN^-] \leq 0.01$ M), a plot of k_{obsd} versus $[SCN^-]$ appears to be linear with a small intercept (Figure 1). The oxidation is hydroxyl independent over the entire experimental range (0.12 M $\leq [OH^-] \leq$ 1.2 M).

From the slope of the plot, the value of the apparent second-order rate constant, k, was found to be (21.7 ± 0.03) M^{-1} s^{-1} at $[SCN^-] \leq 0.01$ M. The intercept (0.014 s^{-1}) is similar to that observed in other systems and can be attributed to reaction of Ag(III) with the solvent and/or the presence of the aquatrihydroxosilver(III) ion.[16]

At higher thiocyanate concentrations, the observed rate constants are also $[OH^-]$ independent, but lower than predicted from the straight line at low concentrations (Table II). However, the data cannot be explained by a change from second to first order, as would be expected if there were a significant preequilibrium association between Ag(III) and SCN^-.

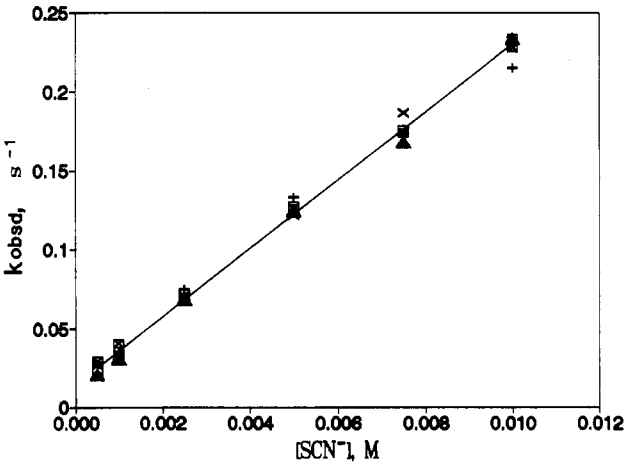

Figure 1. Plot of k_{obsd} vs $[SCN^-]$ at 25 °C, μ = 1.2 M, and low thiocyanate concentration ($[SCN^-] \leq 0.01$ M): (+) $[OH^-]$ = 0.12 M; (□) $[OH^-]$ = 0.3 M; (×) $[OH^-]$ = 0.6 M; (▲) $[OH^-]$ = 0.9 M; (□) $[OH^-]$ = 1.2 M; (—) fitted line.

Table III. Temperature Dependence[a]

T, K	k,[b] M^{-1} s^{-1}	k_{calc}, M^{-1} s^{-1}
288	16.6	16.0
298	24.2	24.9
308	35.6	37.6
318	57.7	55.4
328	80.2	79.7

$\Delta H^{\ddagger} = 28.3 \pm 1.2$ KJ mol^{-1}
$\Delta S^{\ddagger} = -118 \pm 3$ kJ mol^{-1} K^{-1}[c]

[a] $[SCN^-]$ = 0.01 M, $[OH^-]$ = 0.6 M, μ = 1.2 M. [b] $k_{obsd}/[SCN^-]$. [c] Apparent activation parameters. Correction for the proposed mechanism (see Discussion) assuming a constant stoichiometry of 4:1 throughout this temperature range leads to $\Delta S_1^{\ddagger} = -129 \pm 7$ J mol^{-1} K^{-1} for eq 2.

Temperature Dependence. The variation of rate with temperature was determined at $[SCN^-]$ = 0.01 M, $[OH^-]$ = 0.6 M, and 15 °C $\leq T \leq$ 55 °C. Data are listed in Table III. A plot of log (kNh/RT) versus $1/T$, (where T is the absolute temperature and N, h, and R are the Avogadro, Planck, and gas constants) is linear and gives apparent activation parameters of $\Delta H^{\ddagger} = 28.3 \pm 1.2$ kJ mol^{-1} and $\Delta S^{\ddagger} = -118 \pm 3$ J mol^{-1} K^{-1}.

Discussion

Although thiocyanate oxidation has been proposed to involve a one-electron transfer with the production of radicals,[1,2] and $Ag(OH)_4^-$ can undergo one-electron transfer as well,[16] no kinetic

or spectroscopic evidence for any Ag(II) intermediate species was observed in this study. Furthermore, the redox potentials, $E_{Ag(III)/Ag(II)} \simeq 0.74$ V[14] and $E_{SCN^-/SCN\cdot} = 1.61$ V,[2] appear to impose a barrier to one-electron transfer that is incompatible with the observed rate. Although thiocyanate complexes of Au(III) have been reported,[4,32] the absence of a reciprocal hydroxyl dependence and the lack of spectroscopic variations argue against the equilibrium replacement of bound OH^- by SCN^-.[33] On the basis of the above analysis, the following mechanism is proposed for the complete oxidation of SCN^- to SO_4^{2-}.

$$Ag(OH)_4^- + SCN^- \xrightarrow{k_1} Ag(OH)_2^- + SCN^+ + 2OH^- \quad (2)$$

$$SCN^+ + OH^- \rightarrow HOSCN \quad \text{(fast)} \quad (3)$$

$$HOSCN + OH^- \overset{K}{\rightleftharpoons} OSCN^- + H_2O \quad (4)$$

$$Ag(OH)_4^- + OSCN^- \xrightarrow{k_2} Ag(OH)_2^- + OS(O)CN^- + H_2O \quad (5)$$

$$Ag(OH)_4^- + OS(O)CN^- \xrightarrow{k_3} Ag(OH)_2^- + OS(O)_2CN^- + H_2O \quad (6)$$

$$Ag(OH)_4^- + S(O)_2CN^- \xrightarrow{k_4} Ag(OH)_2^- + SO_4^{2-} + OCN^- + 2H^+ \quad (7)$$

$$Ag(OH)_2^- + SCN^- \rightarrow AgSCN + 2OH^- \xrightarrow{SCN^-} Ag(SCN)_2^- \quad (8)$$

Since $K \sim 5 \times 10^8$,[7] the sequence (2)–(4) can be viewed as one reaction with rate constant k_1. Further reaction with $Ag(OH)_4^-$ finally leads to sulfate and cyanate. In Wilson and Harris' mechanism for thiocyanate oxidation by hydrogen peroxide,[12] protonated $OS(O)CN^-$[34] reacts with H_2O_2, forming OCN^- and SO_3^{2-}, which is rapidly oxidized to sulfate. The reaction between $Ag(OH)_4^-$ and sulfite, however, is not sufficiently rapid to explain the absence of SO_3^{2-} at excess SCN^-.[16] Thus, if SO_3^{2-} were produced in the present system, it, and not SO_4^{2-}, should be the final product. In reaction 7, we envisage the simultaneous production of equal amounts of sulfate and cyanate. Although cyanate is metastable and hydrolyzes rapidly in acid, the hydrolysis is very slow in alkaline media; e.g., even at 94 °C, when $[OH^-] = 0.18$ M and $[OCN^-] = 0.018$ M, only 10% of OCN^- decomposes within 1 h.[35]

Reactions 9–12, written for low pH, provide an alternate sequence in which hydrolysis of HOSCN gives sulfate and cyanide,[7] followed by the oxidation of cyanide to cyanate by silver(III).

$$HOSCN + HOSCN \rightarrow HOS(O)CN + SCN^- + H^+ \quad (9)$$

$$HOSCN + HOS(O)CN \rightarrow HOS(O)_2CN + SCN^- + H^+ \quad (10)$$

$$HOS(O)_2CN + H_2O \rightarrow SO_4^{2-} + CN^- + 3H^+ \quad (11)$$

$$Ag(OH)_4^- + CN^- \rightarrow Ag(I) + OCN^- + H_2O + 2OH^- \quad (12)$$

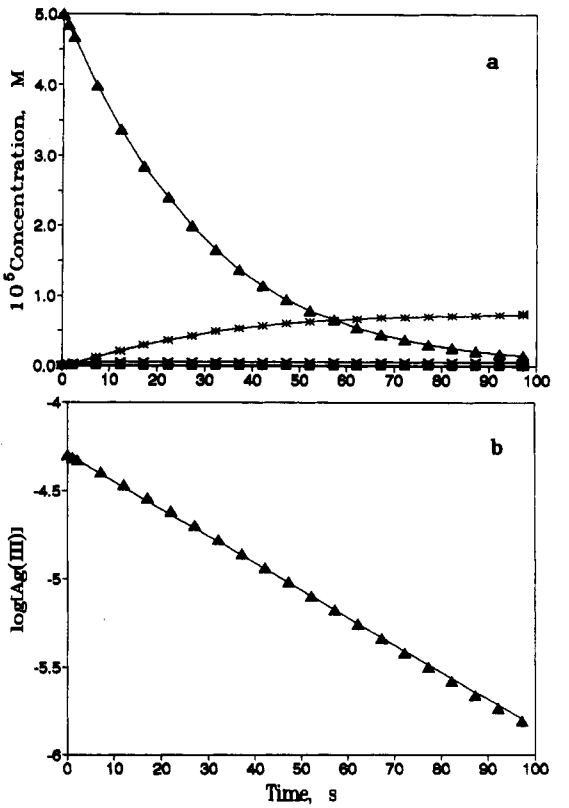

Figure 2. Simulation at $[SCN^-] = 0.001$ M and $Ag(OH)_4^- = 5 \times 10^{-5}$ M, $k_1 = 6.0$ M^{-1} s^{-1}, $k_2 = 4 \times 10^5$ M^{-1} s^{-1}, $k_3 = 1 \times 10^4$ M^{-1} s^{-1}, and $k_4 = 1 \times 10^5$ M^{-1} s^{-1}. (a) Product distribution: (▲) $Ag(OH)_4^-$; (■) $OSCN^-$; (×) $OSOCN^-$; (✱) SO_4^{2-}. (b) $Ag(OH)_4^-$ disappearance: (▲) experimental (–) simulated.

Several factors make this sequence seem unlikely: The decomposition of HOSCN/$OSCN^-$ depends on HOSCN concentration, and indeed $OSCN^-$ is relatively stable in base. Thus, the formation of SO_4^{2-} and CN^- by the sequence (9)–(11) would be slow under our conditions. The second-order rate constant for reaction 12 is 7.7×10^2 M^{-1} s^{-1},[36] and even under the most favorable conditions of our experiments, $[CN^-]$ would be too small to compete with $[SCN^-]$ for $Ag(OH)_4^-$.[37] This rules out any mechanism in which CN^- is an intermediate.

The proposed mechanism requires that reactions 5–7 are all much faster than reaction 2. Since, of the three reacting intermediates, only $OSCN^-$ is stable enough to be prepared and studied, we investigated the reaction of $OSCN^-$ with $Ag(OH)_4^-$. The $OSCN^-$ was prepared from the alkaline hydrolysis of $(SCN)_2$, which was made by reacting bromine with a suspension of $Pb(SCN)_2$ in CCl_4.[7] From the amount of bromine consumed, the concentration of $OSCN^-$ was estimated to be around 10^{-3} M. Kinetic experiments indicate that the second-order rate constant of reaction 5 is at least 2×10^5 M^{-1} s^{-1}.

The production of quantities of sulfate equivalent to that predicted by eq 1 requires that the initial electron-transfer step (reaction 2) is much slower than subsequent steps so that, even at moderate excess of SCN^-, the redox stoichiometry is $\Delta[Ag(III)]/\Delta[SO_4^{2-}] = 4$. This leads to a value of $k_1 \sim k/4 = 5.4$ M^{-1} s^{-1}. The activation entropy, $\Delta S_1^{\ddagger}$, then becomes -129 ± 7 J mol^{-1} K^{-1}. The decrease in observed rate from that predicted by Figure 1 at SCN^- concentrations above 0.01 M can be explained as an increasing competition of reaction 2 for the available $Ag(OH)_4^-$ accompanied by a decrease in stoichiometry.

In order to test the validity of the mechanism, reactions 2–7, we performed a series of numerical simulations using a variety of trial values for the rate constants. Computations were done

(32) Elmroth, S.; Skibsted, L. H.; Elding, L. I. *Inorg. Chem.* **1989**, *28*, 2703.
(33) A reviewer has suggested a mechanism involving equilibrium addition of one and two SCN^- ligands followed by parallel redox paths involving eight and six electron equivalents, respectively. Although the derived rate law is not inconsistent with the data (assuming the first redox step is rate determining), we feel that such a mechanism cannot be supported for reasons which include the following: Rapid, quantitative complexation of virtually all the $Ag(OH)_4^-$ would be required even at very low $[SCN^-]$, but this should give rise to spectral changes and (if four-coordination is maintained) kinetic dependences on hydroxyl ion, both of which are absent. While formation of five- or six- coordinate Ag(III) is possible, $Ag(OH)_4(SCN)_2^{3-}$ would be formed as the trans isomer and would have to reorganize (most likely with a $[OH^-]$ dependence) prior to two-electron redox[24]. The expected two-electron intermediates from the two paths, $OSCN^-$ and $(SCN)_2$, do not explain the change in products since $(SCN)_2$ rapidly hydrolyzes to $OSCN^-$ and SCN^- in alkaline media.
(34) Although their intermediate is formulated as HOOSCN, no evidence is presented that it is a peroxide.
(35) Jensen, M. B. *Acta Chem. Scand.* **1958**, *12*, 778.
(36) Sun, Y.; Kirschenbaum, L. J. Submitted to *Inorg. Chim. Acta.*
(37) In addition, the sequence ending with reaction 12 would give rise to $k_1 = (3/4)k = 16$ M^{-1} s^{-1}. This is inconsistent with the experimental rate, which is only about half of k_{calc} (Table II) at the highest $[SCN^-]$.

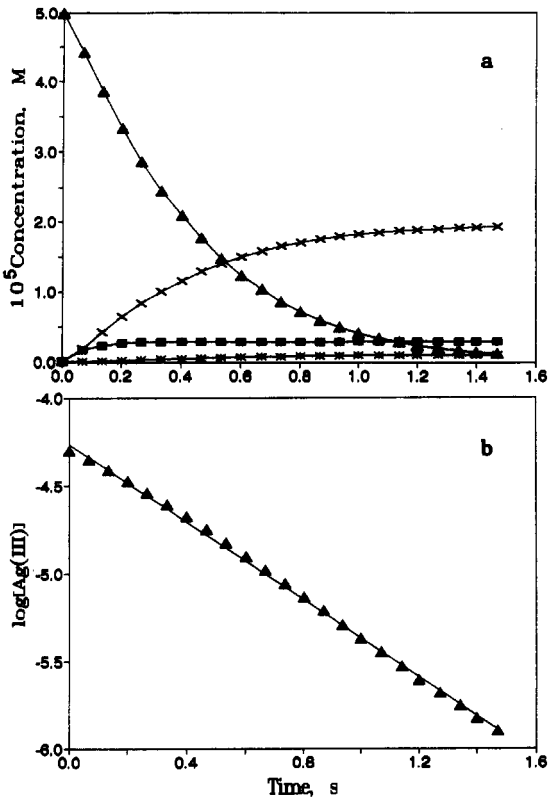

Figure 3. Simulation at $[SCN^-] = 0.2$ M with $[Ag(OH)_4^-]$ and rate parameters as in Figure 2. (a) Product distribution: (▲) $Ag(OH)_4^-$; (■) $OSCN^-$; (×) $OSOCN^-$; (✱) SO_4^{2-}; (b) $Ag(OH)_4^-$ disappearance. (▲) experimental; (—) simulated.

over the experimental concentration range by using the PC version of the program GEAR.[38]

Since close examination of the data reveals some downward curvature even below 0.01 M SCN^- (Figure 1), a value of $k_1 = 6.0\ M^{-1}\ s^{-1}$ and a constant term of $0.013\ s^{-1}$ were chosen for the simulations. A number of sets of trial values were then used for k_2, k_3, and k_4. The most satisfactory results over the entire concentration range were obtained for $k_2 = 4 \times 10^5\ M^{-1}\ s^{-1}$, $k_3 = 1 \times 10^4\ M^{-1}\ s^{-1}$, and $k_4 = 1 \times 10^5\ M^{-1}\ s^{-1}$. Examples of the simulations using these values and $[Ag(OH)_4^-] = 5 \times 10^{-5}$ M are given in Figure 2, for $[SCN^-] = 1 \times 10^{-3}$ M, and Figure 3, for $[SCN^-] = 0.2$ M. For each of the 13 thiocyanate concentrations in Table II, the procedure was as follows: (1) Concentrations of all species were calculated as a function of time (Figures 2a and 3a). (2) The simulated concentration vs time data for $Ag(OH)_4^-$ was plotted as a first-order reaction (Figures 2b and 3b). In every case, the first-order plots gave a satisfactory fit. The rate constants so derived, k_{simul}, are listed in the last column of Table II.

Figure 2a predicts that at low SCN^- concentration, there is quantitative production of SO_4^{2-} and OCN^-; i.e., no reaction intermediates remain after all of the silver(III) has been reduced. Furthermore, the simulated rate constant is very close to the experimental one. On the other hand, at $[SCN^-] = 0.2$ M, a substantial amount of SCN^- is oxidized to $OS(O)CN^-$ (Figure 3a) with a diminished yield of sulfate. Still, there is no significant buildup of other intermediates, and k_{simul} is again close to the experimental value. Figure 4 shows the excellent agreement between observed and simulated rate constants over the entire range of $[SCN^-]$.

The foregoing analysis indicates the feasibility of the proposed reaction scheme, but the values chosen for k_2, k_3, and k_4 are certainly not unique. For example, a satisfactory set of k_{simul} values resulted when k_2 was set at $3 \times 10^4\ M^{-1}\ s^{-1}$ and with $k_3 = k_4 = 1 \times 10^7$. For those conditions, however, the simulated $Ag(OH)_4^-$ data at high $[SCN^-]$ showed deviations from first-order behavior at the beginning of the reaction that were sufficiently pronounced as to be inconsistent with the experimental data. In addition, such a low value of k_2 for the rate of the silver(III)–$OSCN^-$ reaction contradicts the experimental results. It also predicts the formation of significant amounts of $OSCN^-$ at the end of the reaction, but tests for $OSCN^-$ with iodide were negative. Thus, we conclude that the values of k_2, k_3, and k_4 used to construct Figures 2–4 are reasonable and well within an order-of-magnitude of being correct.[39]

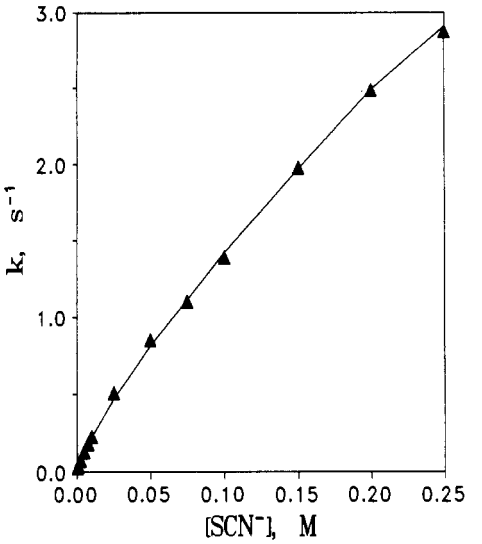

Figure 4. Comparison of experimental and simulated rate constants for $Ag(OH)_4^-$ disappearance: (▲) experimental; (—) simulated.

Figure 3a shows an accumulation of $OS(O)CN^-$ after the completion of the oxidation reaction. In fact, $OS(O)CN^-$ is an unstable species and decomposes by the following sequence:

$$OS(O)CN^- + OS(O)CN^- \xrightarrow{k_{13}} OS(O)_2CN^- + OSCN^- \quad (13)$$

$$OS(O)CN^- + OS(O)_2CN^- + [2OH^-] \xrightarrow{k_{14}} OSCN^- + SO_4^{2-} + OCN^- \quad (14)$$

$$OS(O)_2CN^- + OS(O)_2CN^- + [2OH^-] \xrightarrow{k_{15}} OS(O)CN^- + SO_4^{2-} + OCN^- \quad (15)$$

$$OS(O)CN^- + OSCN^- \xrightarrow{k_{16}} OS(O)_2CN^- + SCN^- \quad (16)$$

$$OS(O)_2CN^- + [2OH^-] \xrightarrow{k_{17}} SO_4^{2-} + CN^- + H_2O \quad (17)$$

Reactions 13–15 have been used by Epstein and co-workers in their simulations of the copper(II)-catalyzed reaction between SCN^- and H_2O_2.[11] Adding reactions 16 and 17, the deprotonated analogues of 10 and 11, provides a mechanism that explains the production of SO_4^{2-} and a mixture of CN^- and OCN^- at high $[SCN^-]$.

Simulations of the complete reaction sequence, reactions 2–7 and 13–17, were performed by using the values chosen by the authors of ref 11 (which used the formulation $OOSCN^-$ rather than $OS(O)CN^-$): $k_{13} = 5 \times 10^2\ M^{-1}\ s^{-1}$, $k_{14} = 1.0 \times 10^3\ M^{-1}\ s^{-1}$, and $k_{15} = 1.0\ M^{-1}\ s^{-1}$. Values of $k_{16} = 1 \times 10^3\ M^{-1}\ s^{-1}$ and $k_{17} = 1 \times 10^{-2}\ s^{-1}$ were also employed. With these parameters, there was substantial conversion of intermediates to CN^- under conditions where CN^- was, indeed, observed experimentally. Smaller values of k_{17} give proportionally higher ratios of OCN^- to CN^-. The time scale of this conversion is sufficiently long that there is no significant effect on Ag(III) disappearance but rapid

(38) Gear, C. W. *Numerical Initial Value Problems in Ordinary Differential Equations*; Prentice Hall: Englewood Cliffs, NJ, 1971. Conversion for PC by R. J. McKinney.

(39) Although the actual product distribution should depend on initial concentrations of both reactants, simulations in which [Ag(III)] was varied (at excess $[SCN^-]$) gave similar results.

enough to explain the positive results within the several minutes required to perform the picric acid test for cyanide.[30b]

The initial reaction between $Ag(OH)_4^-$ and thiocyanate most likely involves a nucleophilic attack of the reductant on the central Ag(III) ion. Like Pt(II), Pd(II), Cu(III), and Au(III), Ag(III) complexes have a low-spin d^8 electron configuration and are square planar. Nucleophilic attack on the Ag(III) site creates a five-coordinate intermediate complex as is characteristic of square-planar ligand substitution and seems important in other $Ag(OH)_4^-$ oxidations.[25] A large negative value of $\Delta S^{\ddagger}$ is common for this associative mechanism. In the intermediate, which is most likely to be S-bound,[40] the SCN^- transfers two electrons directly to the Ag(III), making the stable d^{10} electron configuration of Ag(I) and producing the SCN^+ moiety, which reacts rapidly with OH^-. There are, however, plausible alternatives to reactions 2 and 3, analogues of which have been considered for other $Ag(OH)_4^-$ systems. Direct bimolecular reaction between SCN^- and a bound hydroxyl could produce HOSCN with simultaneous reduction of the metal. A similar path has been proposed in the SCN^- reduction of halogold(III) complexes, resulting in neutral XSCN intermediates.[4] The linear structure of thiocyanate would, however, prohibit such intermediates if SCN and X (or OH) were both bound to the metal. We have discussed this possibility for the reactions of silver(III) and reduced oxoanions, and find that this path is not operative in those cases.[23]

Another alternative to HOSCN production involves the equilibrium replacement of a hydroxyl ion by SCN^- followed by attack of bulk OH^- on the $Ag(OH)_3(SCN)^-$ complex. This combination would be $[OH^-]$ independent as observed. Although this is certainly possible, the lack of evidence for complexation, which *has* been observed in other reactions,[24,26] offers no support for ligand substitution. Finally, questions concerning the actual production of SCN^+ in reaction 2 can be overcome if the nucleophilic attack of SCN^- on silver(III) were rate determining and followed by rapid reaction of OH^- with the five-coordinate intermediate.

Acknowledgment. We wish to thank the Donors of the Petroleum Research Fund, administered by the American Chemical Society, for support of this research.

(40) Golub, A. M.; Köhler, H.; Skopenko, V. V. *Chemistry of Pseudohalides*, Elsevier: Amsterdam, 1986; p 275.

Contribution from the Departments of Chemistry, University of Virginia, Charlottesville, Virginia 22901, University of North Carolina, Chapel Hill, North Carolina 27514, and University of Delaware, Newark, Delaware 19711

Synthesis and Structures of the $[MoFe_6S_6(CO)_{16}]^{2-}$, $[MoFe_4S_3(CO)_{13}(PEt_3)]^{2-}$, and $[Mo_2Fe_2S_2(CO)_{12}]^{2-}$ Ions: High-Nuclearity Mo–Fe–S Clusters as Potential Precursors to Models for the FeMo-Cofactor of Nitrogenase

P. A. Eldredge,[1a] K. S. Bose,[1b] D. E. Barber,[1b] R. F. Bryan,[1b] E. Sinn,[1b,c] A. Rheingold,[1d] and B. A. Averill*,[1b]

Received January 29, 1991

Reaction of $[Mo(CO)_4I_3]^-$ with 2–3 equiv of $[Fe_2S_2(CO)_6]^{2-}$ in THF produces two new Mo–Fe–S–CO clusters, the $[MoFe_6S_6(CO)_{16}]^{2-}$ (I) and $[MoFe_4S_3(CO)_{14}]^{2-}$ (II) ions, both of which have been structurally characterized, the latter as its mono(triethylphosphine) substitution product, $[MoFe_4S_3(CO)_{13}(PEt_3)]^{2-}$ (II-P). Crystallographic data: $(Ph_4As)_2$(I), triclinic, $P\bar{1}$ (No. 2), $Z = 2$, $a = 12.473$ (12) Å, $b = 12.836$ (13) Å, $c = 22.360$ (22) Å, $\alpha = 90.96$ (2)°, $\beta = 97.58$ (2)°, $\gamma = 99.52$ (2)°, $V = 3497$ Å^3, $R = 0.083$, $R_w = 0.094$, 9146 independent reflections with $I > 2.5\sigma(I)$; $(Et_4N)_2$(I), monoclinic, $P2_1/c$ (No. 14), $Z = 4$, $a = 19.275$ (7) Å, $b = 11.940$ (3) Å, $c = 20.975$ (1) Å, $\beta = 90.38$ (4)°, $V = 4827$ Å^3, $R = 0.038$, $R_w = 0.048$, 3872 independent reflections with $I > 3\sigma(I)$; $(Ph_4As)_2$(II-P), monoclinic, $P2_1/c$ (No. 14), $Z = 4$, $a = 18.124$ (4) Å, $b = 15.630$ (3) Å, $c = 24.665$ (5) Å, $\beta = 98.109$ (2)°, $V = 6917$ Å^3, $R = 0.063$, $R_w = 0.063$, 3874 independent reflections with $I > 5\sigma(I)$. Cluster I consists of a low-symmetry (C_1) arrangement of Fe atoms about a highly distorted trigonal-prismatic MoS_6 core, in which all sulfur atoms bridge to two or three Fe atoms. In one direction along a pseudo-2-fold axis of the trigonal prism are two Fe atoms at 2.74 and 2.77 Å from Mo, while the opposite tetragonal face is spanned by a zigzag chain of four Fe atoms, one of which at 2.68 Å is also bonded to Mo. The four-Fe chain contains one relatively long (2.74 Å) Fe–Fe interaction and a single bridging CO ligand, with terminal CO's completing the ligation to each Fe. The structure of I is essentially identical in both salts examined, suggesting that it arises from electronic considerations rather than crystal packing effects. The $MoFe_6S_6$ core stoichiometry of I together with the presence of three Fe atoms 2.7 Å from Mo makes it the closest synthetic approximation yet to the core stoichiometry and structure of the FeMo-cofactor of nitrogenase, suggesting that it may serve as a precursor to models for the FeMo-cofactor via oxidative decarbonylation reactions. Cluster II-P also exhibits a low-symmetry structure in which three new Mo–Fe interactions have been formed within an approximately square-pyramidal $MoS_3(CO)_2$ coordination sphere derived from coordination of two $[Fe_2S_2(CO)_6]^{2-}$ units to Mo with loss of one sulfur atom. The PEt_3 ligand is coordinated to the only Fe atom not bonded to Mo. The average Mo–S distance in both I and II-P is 2.43 Å, consistent with a Mo(II) formulation. Reaction of $[Mo(CO)_5I]^-$ with 1 equiv of $[Fe_2S_2(CO)_6]^{2-}$ results in the formation of cluster II in addition to a new cluster, the $[Mo_2Fe_2S_2(CO)_6]^{2-}$ ion (III), which has been characterized as its Ph_4As^+ salt. Crystallographic data for $(Ph_4As)_2$(III): monoclinic, $P2_1/m$ (No. 11), $Z = 4$, $a = 11.938$ (20) Å, $b = 16.729$ (30) Å, $c = 15.694$ (25) Å, $\beta = 111.45$ (50)°, $V = 2918$ Å^3, $R = 0.062$, $R_w = 0.058$, 3182 independent reflections with $I > 3\sigma(I)$. The structure of III consists of a centrosymmetric distorted octahedral $Mo_2Fe_2S_2$ core containing a planar Mo_2Fe_2 unit, with each Mo coordinated by three terminal CO's, each Fe coordinated by two terminal CO's, and a single CO bridging the Mo and Fe. The average Mo–S distance is 2.54 Å, consistent with a Mo(0) formulation. Plausible schemes for formation of clusters I–III are presented: cluster III arises from reaction of $[Fe_2S_2(CO)_6]^{2-}$ with *two* $[Mo(CO)_5I]^-$ ions; cluster II results from reaction of $[Mo(CO)_4I_3]^-$ with the dimeric disulfide-containing species $[Fe_4S_4(CO)_{12}]^{2-}$ produced in situ by oxidation of $[Fe_2S_2(CO)_6]^{2-}$; and cluster III requires the reaction of $[Mo(CO)_4I_3]^-$ with *both* $[Fe_2S_2(CO)_6]^{2-}$ and $[Fe_4S_4(CO)_{12}]^{2-}$. The implications of clusters I–III for the structure of the FeMo-cofactor of nitrogenase and as potential precursors to detailed models for the FeMo-cofactor are discussed.

The iron–molybdenum cofactor (FeMo-co) of nitrogenase[2] is arguably the most complex metal cluster to occur in biological systems. It contains one molybdenum atom, six to seven iron atoms, eight to ten sulfur atoms,[2,3] and one molecule of homo-

0020-1669/91/1330-2365$02.50/0